RSC Advances

ROYAL SOCIETY OF CHEMISTRY

www.rsc.org/advances

Cite this: DOI: 10.1039/c0xx00000x

www.rsc.org/xxxxxx

ARTICLE TYPE

High Selectivity Up-converted Fluorescence Turn-on Probe for Zn^{2+} Based on PAMAM Hydroxy-Naphthalene Schiff-bases (C=N) Half-organic Quantum Dots

Yan Ji,[a] and Ying Qian*[a]

Received (in XXX, XXX) Xth XXXXXXXXX 20XX, Accepted Xth XXXXXXXXX 20XX
DOI: 10.1039/b000000x

Dendrimer PNS-G0 including Schiff-base imine (C=N) realize high selective and common fluorescence (λex=400 nm) or up-converted fluorescence (λex=800 nm) turn-on effect to qualitatively and quantitatively detect zinc ion (Zn^{2+}). The PNS-G0+Zn^{2+} complex (C=N_Zn_O) fluorescence emission parts were firstly proposed as the Half-organic Quantum Dots (HOQDs). The HOQDs probe PNS-G0 for Zn^{2+} by coordination method based on imine isomerization (inhibited) mechanism, which has potential applications in biological imaging, analytical chemistry, and optical physics areas.

1. Introduction

Zinc is an important element in biological tissues, for many enzymes and proteins included zinc ion (Zn^{2+}) [1, 2]. Therefore the qualitative and quantitative analysis for Zn^{2+} in the tissues, and detecting the positions of Zn^{2+} were important in the study of biological processes. The fluorescence probe molecules were the simple, sensitive, fast, and efficient tools for detecting Zn^{2+} ions [3]. The two-photon absorption-induced up-converted fluorescence probe for Zn^{2+} were cared in biology, chemistry, even physics areas [4].

There were several probe mechanisms have been reviewed [5], such as photoinduced electron transfer (PET) [6], excimer/exciplex formation [7], intramolecular charge transfer (ICT) [8], metal-ligand charge transfer (MLCT) [9], fluorescence resonance energy transfer (FRET) [10], twisted intramolecular charge transfer (TICT) [11], electronic energy transfer (EET) [12], aggregation-induced emission (AIE) [13], and excited-state intramolecular proton transfer (ESIPT) [14]. Recently, the Schiff-base imine (C=N) isomerization phenomena were cared and have been used in the design and synthesis of new type probe [15]. The Schiff-base imine (C=N) gave no or weak fluorescence for the isomerization phenomena. If the imine isomerization was inhibited by complexing with metal ions through coordination bonds, then the imine can give fluorescence emission [5]. These C=N isomerization-based probes can realize fluorescence turn-on effect in detecting various metal ions (e.g. Mg^{2+}, Cu^{2+}, Cd^{2+}) [16].

Based on this strategy, the dendrimer PNS-G0 (Scheme 1) including imine (C=N) group was synthesized from poly-(amido-amine) generation zero (PAMAM G0) and 2-hydroxy-1-naphthaldehyde by Schiff base reaction, which can probe Zn^{2+} ions. PNS-G0 have PAMAM-G0 center core with many amines (tertiary amine, amide, and imine). And PAMAM have intramolecular holes between flexible chains, which can complex with metal ions and package nano particles or small molecules, even realize drugs delivery. And the PAMAM can emission fluorescence after storing or oxidation in air [17], which was caused the interests in related areas such as fluorescence probe design. The end group of PNS-G0 was 2-hydroxy-1-naphthaldehyde. The hydroxyl was reserved for forming coordination bond. The aldehyde can react with amine of PAMAM by Schiff base condensation reaction, which can form imine (C=N) group for the using of C=N isomerization mechanism.

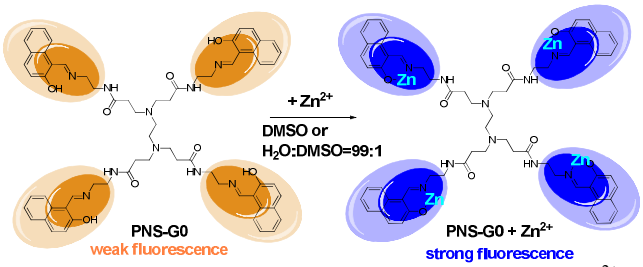

Scheme 1 the structures of PNS-G0 and its complex with Zn^{2+}

The semiconductor nano-particles were known as quantum dots (QDs) [18]. QDs are characterized by large Stokes shifts, broad absorption bands, and narrow, size-dependent emission bands without a significant red tail. The multiple color QDs can be excited using a single laser excitation wavelength [19]. The size-dependent emission of QDs is the result of a quantum confinement effect (QCE). The QCE occurs when the size of the exciton (exciton Bohr radius, B) exceeds the physical size of the semiconductor nano crystal (D) [20]. Semiconductor nano crystals exhibit particularly interesting properties when the exciton is

strongly confined (D < 2B) [21] and outperform fluorescent dyes in terms of brightness and photo stability [22]. Inorganic QDs composited with organic molecules form a new kind of QDs type, as Half-organic Quantum Dots (HOQDs) were firstly named. The HOQDs have been involved in recently research, such as Cystene thiol QDs [23] and PAMAM thiol modified QDs [24], and other half organic parts QDs [25]. In this paper, the imine_Zn_hydroxyl (C=N_Zn_O) complex HOQDs were discussed.

2. Results and Discussions

2.1. Selectivity of Probing Zn^{2+}

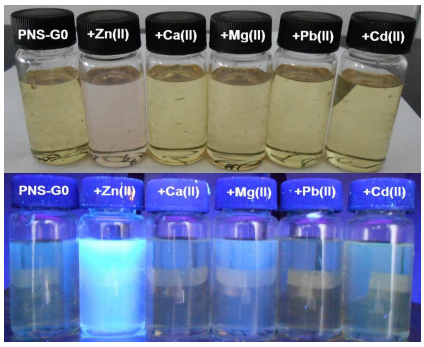

Figure 1 The photographs of probe PNS-G0 and its complex with different metal ions (Zn^{2+}, Ca^{2+}, Mg^{2+}, Pb^{2+}, Cd^{2+}) in DMSO (5×10^{-5} mol/L). The up photograph was in room light; the down photograph was in UV light (365 nm).

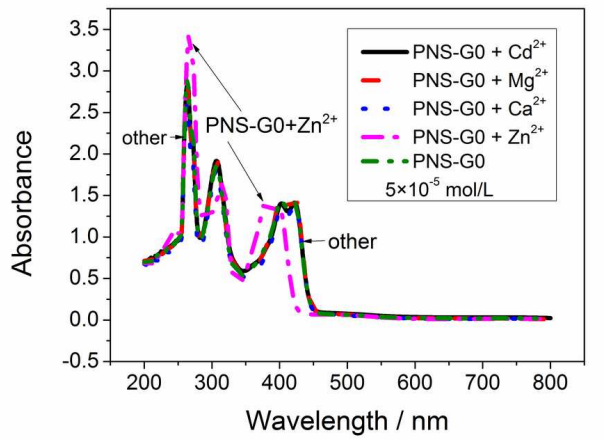

Figure 2 The UV-vis absorption spectra of PNS-G0 (5×10^{-5} mol/L) and PNS-G0 complex with different metal ions (Zn^{2+}, Cd^{2+}, Mg^{2+}, Ca^{2+}) (1×10^{-4} mol/L)

Figure 1 gave the photographs of PNS-G0 and its complex with several metal ions in DMSO solutions. From Figure1, the PNS-G0 gave weak emission under UV light. PNS-G0 gave strong blue fluorescence after complex with Zn2+. And PNS-G0 complex with other metal ions (Ca^{2+}, Mg^{2+}, Pb^{2+}, and Cd^{2+}) gave weak fluorescence. The Figure 1 can show the fluorescence selectivity of PNS-G0 for probe Zn^{2+} distinguished by eyes.

Figure 2 give UV-vis absorption spectra of the PNS-G0 and PNS-G0 complex with Zn^{2+} and other metal ions. The main absorbance peaks were at 250 nm, 300 nm, and 400 nm. Compared the UV-vis absorption spectra of the PNS-G0 and PNS-G0 complex, the Zn^{2+} ions complex have higher UV-vis absorbance peaks at 250 nm and have lower UV-vis absorbance peaks at 300 nm than that of other metal ions complex. The Zn^{2+} ions complex UV-vis absorbance peaks have 380 nm peaks and show blue shift compared with other metal ions complex. The UV-vis absorption spectra shows the spectra of PNS-G0+Zn^{2+} complex different with other metal ions. It can be seen that the Zn^{2+} complex with PNS-G0 change the n-π* and π-π* transition absorbance, which show the unique absorbance characters of Zn^{2+}+PNS-G0 complex different from UV-vis absorption spectra of PNS-G0 and the other metal ions complex.

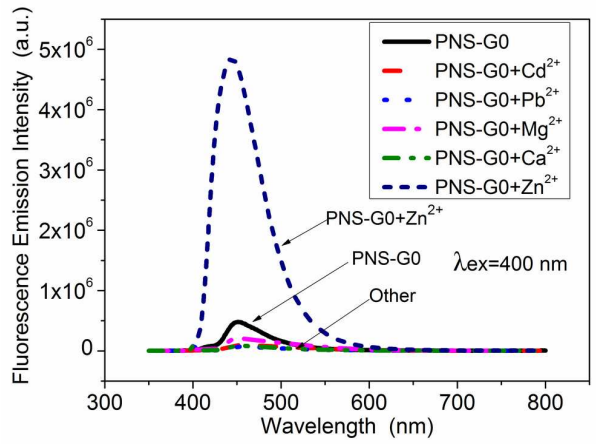

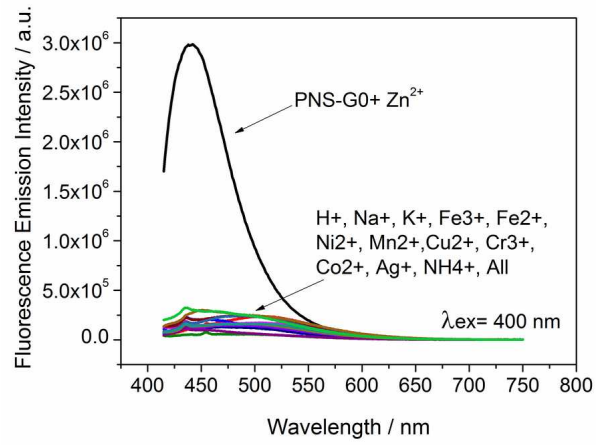

Figure 3 The fluorescence emission of probe PNS-G0 (5×10^{-5} mol/L) and its complex with different metal ions (Zn^{2+}, Ca^{2+}, Mg^{2+}, Pb^{2+}, Cd^{2+}, Mn^{2+}, Fe^{3+}, Fe^{2+}, Ni^{2+}, Cu^{2+}, Co^{2+}, Cr^{3+}, Ag^{+}, H^{+}, NH_4^{+}, Na^{+}, K^{+}) (1×10^{-4} mol/L) in DMSO (excited under 400 nm wavelength light)

The fluorescence emission spectra in Figure 3 show that the PNS-G0 gave ten times fluorescence enhanced after complex with Zn^{2+}, while other metal ions complexes gave very weak fluorescence emission. Employing sulfuric acid quinine fluorescence reference method test the fluorescence quantum yield Φ of PNS-G0 and its metal ions complexes gave Φ_{PNS-G0}=0.06; $\Phi_{PNS-G0+Ca2+}$=0.01; $\Phi_{PNS-G0+Mg2+}$=0.04; $\Phi_{PNS-G0+Pb2+}$=0.01; $\Phi_{PNS-G0+Cd2+}$=0.02; $\Phi_{PNS-G0+Zn2+}$=0.73, which show the PNS-G0

complex with Zn^{2+} gave the highest Φ about ten times than that of others. Figure 4 two-times give the PNS-G0 complex in mixed solvent H_2O/DMSO=99:1 and Zn^{2+} complex have higher emission intensity than other metal ions complex. The introduction of water solvent can enhance the biocompatibilities, and PNS-G0 show well fluorescence selectivity in this mixed solvent. It can be got from Figure 1 to Figure 4 that the probe PNS-G0 realized fluorescence enhanced and fluorescence turn-on effect on detecting Zn^{2+}, and show high selective by comparing with other metal ions.

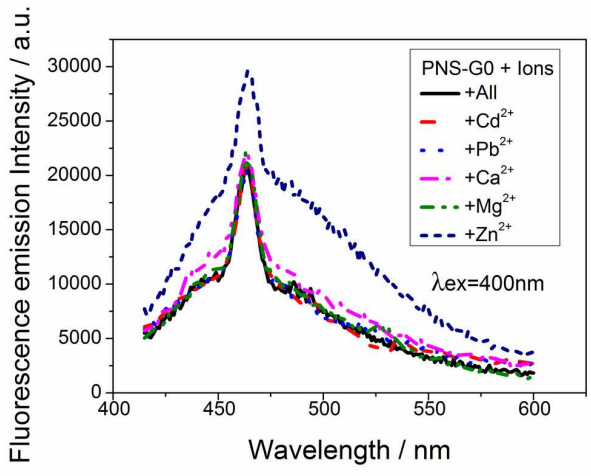

Figure 4 The fluorescence emission of probe PNS-G0 (1×10^{-6} mol/L)and its complex with different metal ions (Zn^{2+}, Ca^{2+}, Mg^{2+}, Pb^{2+}, Cd^{2+}) (1×10^{-4} mol/L) in mixed solvent H_2O/DMSO=99:1 (excited under 400 nm wavelength light)

2.2 Quantitative Probing Zn^{2+}

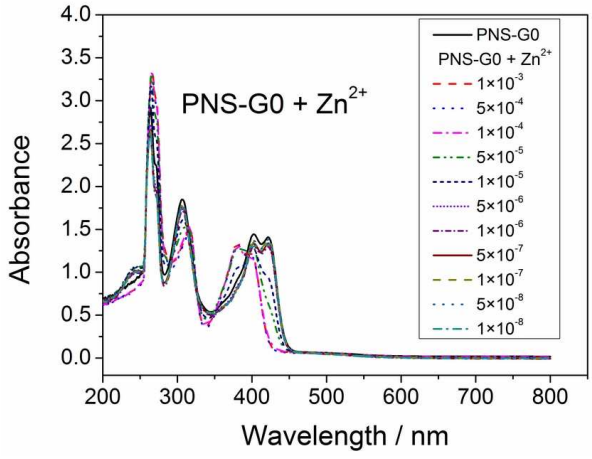

Figure 5 The UV-vis absorption spectra of PNS-G0 (1×10^{-4} mol/L) and PNS-G0 complex with different concentration [Zn^{2+}] (mol/L).

The UV-vis absorption spectra of PNS-G0 and complex with different concentration Zn^{2+} in solvent DMSO show in Figure 5. The UV-vis absorbance peaks become higher at 250 nm and lower at 300 nm along with the increasing of concentration Zn^{2+}. It was notified that the UV-vis absorbance peaks at about 400 nm gave blue shift along with the increasing of concentration Zn^{2+}, which show the Zn^{2+} influence the π-π* conjugated imine-naphthalene absorbance after complex with PNS-G0.

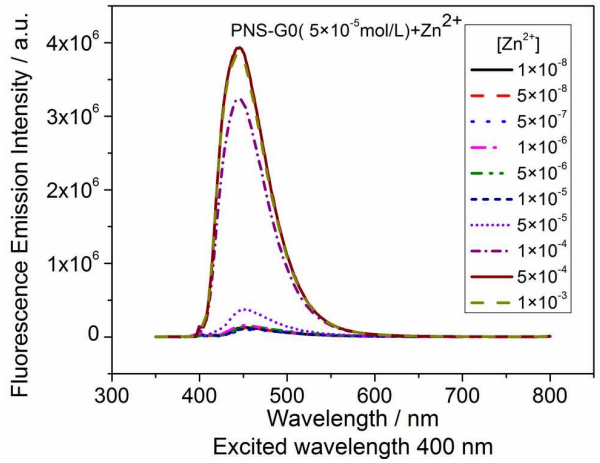

Figure 6 The fluorescence emission spectra of PNS-G0 (5×10^{-5} mol/L) and PNS-G0 complex with different concentration [Zn^{2+}] in DMSO.

The Figure 6 shows the fluorescence emission spectra of PNS-G0+Zn^{2+} complex with different concentration Zn^{2+} in DMSO. The PNS-G0 keeps at 5×10^{-5} mol/L and added in Zn^{2+} DMSO solution with concentrations from 1×10^{-8} mol/L to 1×10^{-3} mol/L. The fluorescence increased along with the increasing of [Zn^{2+}] concentration.

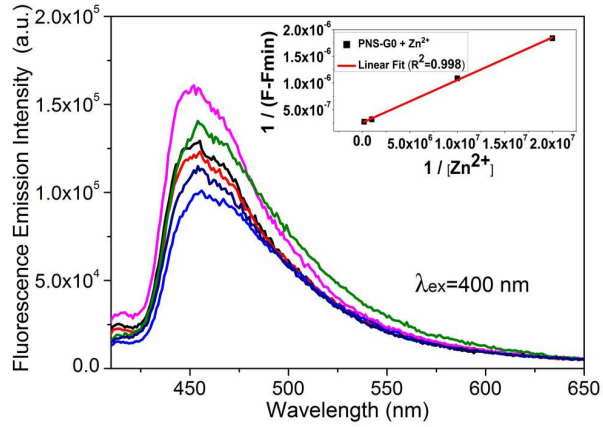

Figure 7 The fluorescence emission spectra of PNS-G0 (5×10^{-5} mol/L) added with Zn^{2+} (1×10^{-8} mol/L ~5×10^{-6} mol/L) in DMSO (insert 1/(F-Fmin) vs. 1/[Zn^{2+}] figure, F was fluorescent emission spectra integrate area) excited under 400 nm wavelength light. Fmin was the minimum [Zn^{2+}] added samples fluorescence spectra integrate area.

The PNS-G0 can qualitatively detect the Zn^{2+} and also can quantitatively detect the Zn^{2+} as shown in Figure 7. The insert graph in Figure 7 shows the well linear relationship of PNS-G0 probing the [Zn^{2+}] (range from 1×10^{-8} mol/L to 5×10^{-6} mol/L). From the data in Figure 5, the approximate binding constant of

the single branch of PNS-G0 was K1 ≈ 2×10^3 M^{-1} by equation [26] ($\Delta A/L = (([Dt]\ K1\ \Delta\varepsilon\ [M])/(1+K1\ [M]))$. The fluorescence spectra in Figure 8 gave the PNS-G0 qualitatively detect the $[Zn^{2+}]$ in mixed solvent H_2O/DMSO=99:1. The 1/(F-Fmin) vs. $1/[Zn^{2+}]$ [26c] have well linear relationship. It can be got from Figure 5 to Figure 8 that the probe PNS-G0 realized qualitatively detecting the Zn^{2+} by fluorescence method. The organic solvent using and near two times selected sign in water/DMSO mixed solvents show the dyes gave inconvenience in biological imaging, which need further modify.

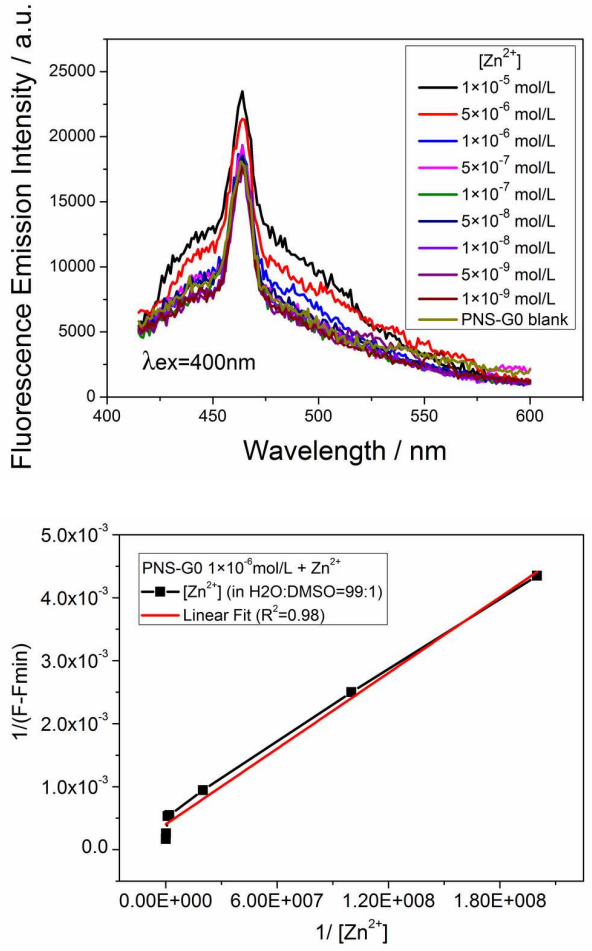

Figure 8 The fluorescence emission spectra (left) of PNS-G0 (1×10^{-6} mol/L) and PNS-G0 complex with different concentration $[Zn^{2+}]$ in mixed solvent H_2O/DMSO=99:1. 1/(F-Fmin) vs. $1/[Zn^{2+}]$ figure (right), F was fluorescent emission spectra integrate area, Fmin was the minimum $[Zn^{2+}]$ added samples fluorescence spectra integrate area.) (Excited under 400 nm wavelength light)

2.3 Up-converted Fluorescence Spectra

The up-converted fluorescence (anti-Stokes emissions) can realize long wavelength excitation and short wavelength emission [27]. After the advent of lasers, the two- and even three-photon absorption-induced frequency up-converted fluorescence in organic dye materials could be observed by using pulsed laser excitation[28]. Long excited wavelength of up-converted fluorescence can realize reduced optical damage, deep penetration, dark fields imaging, high resolution three dimension display, and other advantages of probes used in biology tissues [29].

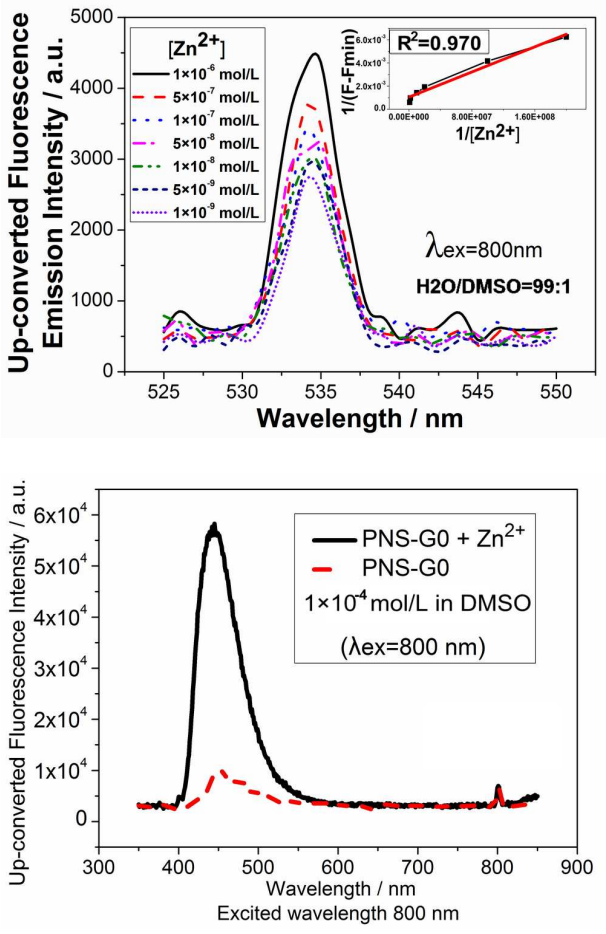

Figure 9 Up-converted fluorescence emission spectra of PNS-G0 (1×10^{-6} mol/L) and complex with different concentration Zn^{2+} in solvent H_2O/DMSO=99:1 (above figure) and up-converted fluorescence spectra of PNS-G0 compared complex with Zn^{2+} in DMSO (below figure). insert 1/(F-Fmin) vs. $1/[Zn^{2+}]$ figure, F was fluorescent intensity, R^2=0.97). The excited wavelength was 800 nm. Fmin was the minimum $[Zn^{2+}]$ added samples fluorescence intensity.

Figure 9 shows that the emission peaks at 535 nm were the results excited at 800 nm wavelength light, which attributed to two-photon mechanism up-converted fluorescence. The up-converted fluorescence emission spectra of PNS-G0 and complex PNS-G0+Zn^{2+} realize turn-on effect in DMSO (insert in Figure 9). The up-converted fluorescence properties of PNS-G0 excited under 800 nm also can qualitatively and quantitatively detect the Zn^{2+} shown in Figure 9. And the introduce water mixed with 1% DMSO as solvent must extend PNS-G0 application in the imaging of cells or tissue.

Figure 10 gave the up-converted fluorescence emission spectra of probe PNS-G0 and its complex with different metal ions (Zn^{2+}, Ca^{2+}, Mg^{2+}, Pb^{2+}, Cd^{2+}) in mixed solvent H_2O/DMSO=99:1 excited under 800 nm wavelength light. Figure 10 show the PNS-

G0+Zn^{2+} complex has higher fluorescence emission peaks than that of PNS-G0 and other metals ions complex excited at 800 nm wavelength light. It can be got from Figure 10 that the probe PNS-G0 realized near two-times selective detect Zn^{2+} compared with other metal ions by up-converted fluorescence spectra.

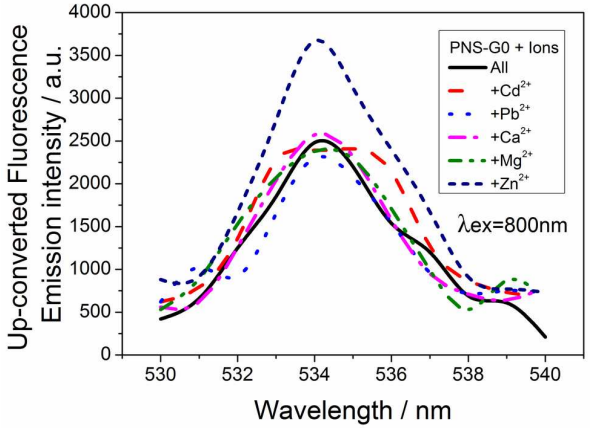

Figure 10 The up-converted fluorescence emission spectra of probe PNS-G0 (1×10^{-6} mol/L) and its complex with different metal ions (Zn^{2+}, Ca^{2+}, Mg^{2+}, Pb^{2+}, Cd^{2+}) (1×10^{-4} mol/L) in mixed solvent H_2O/DMSO=99:1 (excited under 800 nm wavelength light)

The Figure 9 and Figure 10 spectra show the realizing up-converted fluorescence under common linear light source. The experiments were taken by FluoroMax-4 spectrofluorometer from excitation source xenon, continuous output, ozone-free lamp (150 W) at room temperature (~20□), which replaced the laser instruments. The linear light source excitied organic molecules to give up-converted fluorescence emission phenomna were firstly tested. The FluoroMax-4 spectrofluorometer was the common fluorescence testing instruments. The light source was linear, which different with the laser source. The linear source excited up-converted fluorescence organic molecules included PNS-G0+Zn^{2+} dendrimers, which might be cared in chemistry, physics, and biology areas.

Up-converted fluorescence has three mechanisms [30]: the first was second-harmonic generation, the second was two-photon absorption, and the third was photon avalanche [31] process. The Figure 2 and Figure 5 gave the UV-vis absorption spectra that show there were no linear absorbance at 800 nm, which means there exits nonlinear absorbance to produce fluorescence emission under 800 nm excited wavelength. Figure 9 show the peaks of the emission peaks at about 535 nm were attributed to two-photon absorption-induced up-converted fluorescence mechanism.

From the Figure 9 with the insert figure show the PNS-G0 complex with Zn^{2+} emission fluorescence at about 535 nm in mixed solvent H_2O/DMSO=99:1 and emission at 450 nm in DMSO solvent (excited under 800 nm wavelength light), which have about 95 nm shifts. The mainly possibility was the influence of solvent. The solvent effect parameters including polarity, dielectric constant (ε_0), refractive index (n), orientation polarizability (Δf) influence the PNS-G0 complex fluorescence emission. The different dipole-dipole action of solvent make the PNS-G0 in different environments, which make the excited-states and dipole moments changed to give different fluorescence emission peaks. The solvent also have energy transfer to the PNS-G0, under the outer light excited, which might influence the fluorescence emission positions. The different solvent effect of water and DMSO influence on PNS-G0+Zn^{2+} complex at 800 nm excited wavelength forming the 95 nm shifts of up-converted fluorescence emission peaks shown in Figure 9 and the insert figure.

2.4 Imine (C=N) Isomerization Mechanism

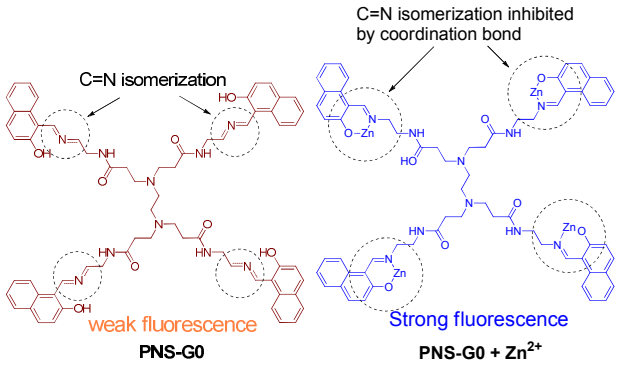

Figure 11 Schiff-base imine (C=N) isomerization inhibited mechanism

Considered the mechanism (Figure 11), Schiff base imine (C=N) exits isomerization with forming the single/double bonds resonance structures, which make the energy of molecular excited states released through non-radiative processes in microscopic, and gave no or weak fluorescence in macroscopic. But if the C=N isomerization inhibited by complex with metal ions through coordination bonds, then the imine C=N can enhance fluorescence emission ratios. PNS-G0 with imine C=N bonds were used this mechanism to probe for Zn^{2+}. Probe PNS-G0 gave weak fluorescence before complex with Zn^{2+}. When detecting the Zn^{2+}, the imine (C=N), hydroxyl (HO-), and amines of PAMAM form coordination bonds with ions. Then the C=N_Zn_O parts with naphthalene gave strong fluorescence emission. The imine (C=N) was locked by coordination bonds with Zn^{2+} and then the naphthalene (as Donor) and imine (C=N) (as Accepter) form D-A (push-pull type) dipole emission unit. This dipole unit was coplanar conjugated group and can enhance nonlinear optical properties, such as two-photon up-converted fluorescence emission. These make PNS-G0 can emission up-converted fluorescence and forming turn-on effect when probing Zn^{2+} ions.

2.5 Half-organic Quantum Dots (HOQDs)

PNS-G0 matched Zn^{2+} gave strong fluorescence emission, which was different from other metal ions PNS-G0 complex. The fluorescence spectra in Figure 3, 4, 10 proved the PNS-G0 have well selectivity on Zn^{2+}. These show the PNS-G0 complex with Zn^{2+} to form half-inorganic (Zn ions)+half-organic (hydroxyl-naphthalene imine) structures, which were unique fluorescence emission groups that were different from other metal ions PNS-

G0 complex.

Figure 4, 8, 9 show the sharp emission peaks in mixed solvent H_2O/DMSO=99:1 were different with the spectra in DMSO solvent. Figure 4, 8 peaks ranges were from 455 nm to 475 nm about 20 nm wide. The PNS-G0 gave enhanced emission at these narrow ranges. For example in Figure 4, the one sharp peaks from 12500 to 24000 a.u., which increased 11500 a.u.. The excited wavelength also influences the sharp shape of emission peaks. At the excited wavelength 400 nm (Figure 4, 8), complex gave sharp peaks with range about 20 nm (455 nm to 475 nm); at the excited wavelength 800 nm (Figure 9), complex gave sharp peaks with range about 10 nm (530 nm to 540 nm).

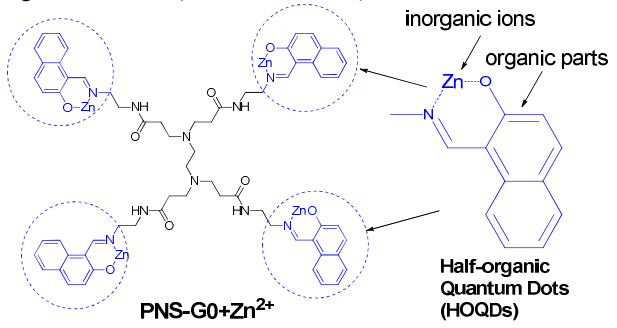

Figure 12 The Half-organic Quantum Dots (HOQDs) of C=N_Zn_O

The PNS-G0+Zn^{2+} complex (Figure 12) has ZnO unit. ZnO was the traditional typical quantum dots [32]. The sharp type of emission peaks also appeared in photoluminescence spectrum of the ZnO-PAMAM-G3 nano composite dispersed in water after excitation at 350 nm room temperature[33]. These sharp peaks may concern with PAMAM, Zn element, water solvent, and excited wavelength, even nano states of molecules or particles. This PNS-G0+Zn^{2+} complex narrow emission peaks were similar with fluorescence quantum dots (QDs) narrow emission band characters. PNS-G0+Zn^{2+} have sharp peaks in the fluorescence emission spectra, emission peaks narrow, and the PNS-G0 complex with Zn^{2+} that has inorganic metal ions and organic hydroxyl+imines ligands. So this PNS-G0+Zn^{2+} complex has organic conjugated parts and ZnO QDs parts, which was firstly called as Half-organic Quantum Dots (HOQDs).

The HOQDs gave different sharp peaks shapes and different emission position under the different excited wavelength or solvents. Solvent effect and environment of complex molecules distribute in solution co-act on the forming of sharp peaks. The complex gave sharp emission peaks in mixed solvent H_2O/DMSO=99:1 and gave smooth emission peaks in DMSO solvent, which show the environment and states of the complex influence the sharp shape of emission peaks. The solvent environment including polarity, dielectric constant (ε0), refractive index (n), orientation polarizability (Δf) influence the peaks shapes. The states of complex might be the other influence elements. The PNS-G0 was well dissolved in DMSO but difficult in water. Then the H_2O/DMSO=99:1 mixed solvent system were used to dissolved PNS-G0 to test fluorescence properties for simulated the biological environment. The PNS-G0 with Zn^{2+} formed ZnO unit complex in these mixed solvent. The ZnO connected with C=N and naphthalene make these HOQDs show the narrow emission bands character, then peaks shape were sharp in these mixed H_2O/DMSO=99:1 solvent.

The PNS-G0 has primary amine, amide, imine, hydroxyl, that all can take part in complex, so the complex moles ratios with Zn^{2+} were difficult to show clear. Figure 13 give the predicted structures, which were used for quantum chemical calculations. These kinds of HOQDs (Figure 13: **P-02** and **P-03**) all have inorganic metal ions and organic parts, which gave fluorescence emission, similar with traditional QDs. The HOQDs have organic parts that can give these QDs more organic characters, such as dissolubility, reacted activity, biocompatibility, and more chemical modified properties. PNS-G0+Zn^{2+} complex have Zn^{2+}_imine fluorescence emission groups that can used as probed label. The PAMAM cores also can emission fluorescence at some situation, and can package nano particles or drug to be deliver. These gave (C=N_Zn_O) HOQDs more diversity on application.

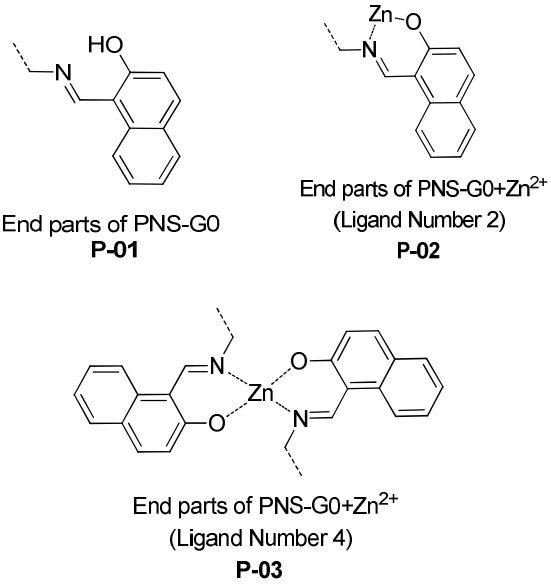

Figure 13 The end parts of PNS-G0 and PNS-G0+Zn^{2+} complex (**P-01** is the end parts of PNS-G0; **P-02** is the predicted end parts of PNS-G0+Zn^{2+} (ligand number 2); **P-03** is the predicted end parts of PNS-G0+Zn^{2+} (ligand number 4)

The HOQDS have the organic parts and inorganic parts. PNS-G0+Zn^{2+} HOQDs have Zn ions as the inorganic parts, and imine conjugated with hydroxyl-aphthalene cycle as organic parts. The QDs have main characters were quantum confinement effect (QCE). HOQDs have quantum confinement effect determined from the Bohr radius compared with the size of in/organic quantum parts. Figure 13 gave the end parts of PNS-G0 (**P-01**) and PNS-G0+Zn^{2+} (**P-02**, **P-03**).

The Figure 14, Figure 15, and Figure 16 gave the molecules orbits of **P-01**, **P-02**, and **P-03**. The calculation used the time-dependent density functional theory (TD_DFT) b3lyp 6-31g methods by *Gaussian 09* software package [34]. Table 1, 2, 3 list the absorption and emission spectra of **P-01**, **P-02**, **P-03** in gas phase vacuum calculated by TD_DFT b3lyp/6-31g method. S0→S1 was the absorption states; S1→S0 was the emission states.

.

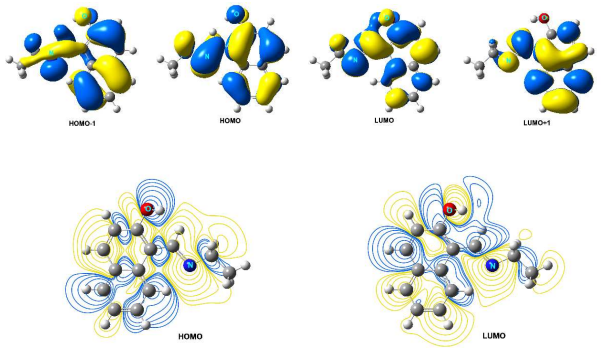

Figure 14 The molecules orbits cloud and contour figures (HOMO-1, HOMO, LUMO and LUMO+1) of **P-01** (end parts of PNS-G0).

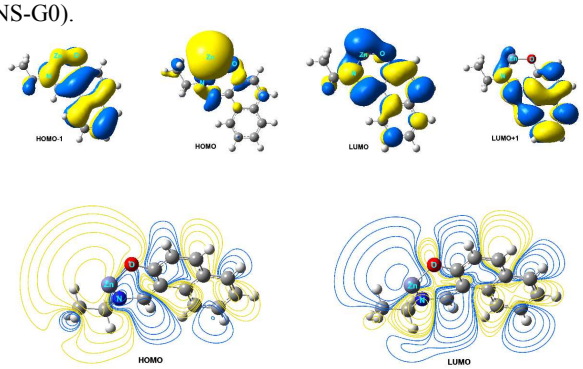

Figure 15 The molecules orbits cloud and contour figures (HOMO-1, HOMO, LUMO and LUMO+1) of **P-02** (end parts of PNS-G0+Zn^{2+}, ligand number 2).

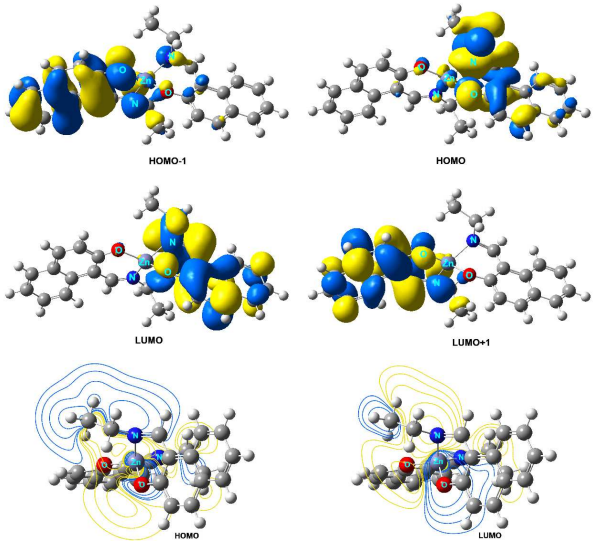

Figure 16 The molecules orbits cloud and contour figures (HOMO-1, HOMO, LUMO and LUMO+1) of **P-03** (end parts of PNS-G0+Zn^{2+}, ligand number 4).

These HOQDs have two Bohr radius directions: one is the Bohr radius of Zn ions expend to free space; the other is the imine naphthalene hydroxyl organic conjugated parts. The former was same as the traditional QDs Bohr radius. The latter was π-conjugated organic cycles, which expend the electronic cloud by real atom parts that can be seen the real atom part Bohr radius. The free space expend Bohr radius and real organic conjugated part Bohr radius form the characters of HOQDs self properties. So the HOQDs might become a new type of QDs to be given more cared

The **P-01** HOMO, LUMO contour figures show the electronic clouds were distributed at the close side of molecules. The **P-02** and **P-03** HOMO, LUMO contour figures show the electronic clouds at the Zn^{2+} parts were distributed far away from the Zn atom, which may regard as Bohr radius gave values about ≈10 Bohr (B). The C=N_Zn_O six members cycle were the main parts of HOQDs, which gave size values about ≈6 Bohr (D). This HOQDs obey the D<2B, which show the quantum confinement effect.

Table 1. The absorption and emission spectra of **P-01** in gas phase vacuum calculated by TD_DFT b3lyp/6-31g method.

Electron transition [a]	Energy (eV)	Calculated wavelength (nm)	Main transition configuration	Oscillator strength *f*
S0→S1	2.857	433.93	HOMO→LUMO: -0.62210 HOMO-1→LUMO: 0.11833 HOMO-3→LUMO: 0.31203	0.2138
S0→S1	2.940	421.68	HOMO→LUMO:0.30241 HOMO-1→LUMO: 0.43256 HOMO-2→LUMO: 0.33605 HOMO-3→LUMO: 0.32663	0.0794
S0→S1	3.124	396.87	HOMO→LUMO+2: 0.17661 HOMO-1→LUMO: -0.28034 HOMO-2→LUMO: 0.58927 HOMO-3→LUMO: -0.17738	0.0395
S1→S0	2.857	433.93	LUMO→HOMO: 0.12852	0.2138

[a] S0→S1 was the absorption states of **P-01;** S1→S0 was the emission states of **P-01**

Table 2. The absorption and emission spectra of **P-02** in gas phase vacuum calculated by TD_DFT b3lyp/6-31g method.

Electron transition [a]	Energy (eV)	Calculated wavelength (nm)	Main transition configuration	Oscillator strength *f*
S0→S1	0.220	5624.95	HOMO→LUMO: -1.03080	0.0049
S0→S1	1.967	630.12	HOMO→LUMO+1: 0.93489 HOMO-1→LUMO: 0.18387 HOMO-1→HOMO: -0.26499	0.0036
S0→S1	2.113	586.72	HOMO-1→HOMO: 0.61623 HOMO-4→HOMO: -0.12701 HOMO→LUMO+1: 0.31794 HOMO-1→LUMO: -0.67219 HOMO-4→LUMO: 0.13763	0.0013
S1→S0	0.220	5624.95	LUMO→HOMO: 0.26503	0.0049

[a] S0→S1 was the absorption states of **P-02;** S1→S0 was the emission states of **P-02**

Table 3. The absorption and emission spectra of **P-03** in gas phase vacuum calculated by TD_DFT b3lyp/6-31g method.

Electron transition [a]	Energy (eV)	Calculated wavelength (nm)	Main transition configuration	Oscillator strength *f*
S0→S1	1.321	938.47	HOMO-2→LUMO: -0.14309 HOMO→LUMO: 0.69075	0.0167
S0→S1	2.297	539.66	HOMO-1→LUMO: 0.70362	0.0460
S0→S1	2.318	534.72	HOMO→LUMO+1: 0.70463	0.0030
S1→S0	1.321	938.47	LUMO→HOMO: -0.13198	0.0167

[a] S0→S1 was the absorption states of **P-03;** S1→S0 was the emission states of **P-03**

3. Experimental Section

PNS-G0 was synthesized from PAMAM-G0 (Figure 17) and 2-hydroxy-1-naphthaldehyde by Schiff base reaction. PNS-G0 acted with the different metal ions (Zn^{2+}, Ca^{2+}, Mg^{2+}, Pb^{2+}, Cd^{2+}, Mn^{2+}, Fe^{3+}, Fe^{2+}, Ni^{2+}, Cu^{2+}, Co^{2+}, Cr^{3+}, Ag^{+}, H^{+}, NH_4^{+}, Na^{+}, K^{+}) in DMSO and water+DMSO (99 : 1) mixed solvent to test the selectivity by UV-vis absorption and fluorescence spectra. Testing PNS-G0 acted with the different concentration Zn^{2+} ions solution for sensitivity and quantitative detecting. The (up-converted) fluorescence was tested for the turn-on effects of probing for Zn^{2+}.

3.1 The synthesis of polyamides-amine (PAMAM-G0) dendrimers[35]

Methyl acrylate (MA) and ethylenediamine (EDA) were used as substrates. The Michael-addition of amine groups in EDA to MA under 50 □ in methanol solution (affords the dendritic product of -0.5 generation (G) with ester groups terminated). The amidation of the terminal ester groups of -0.5G dendrimer from dissolving in methanol solution by excessive EDA under 50 □ (affords the 0G dendrimer with terminal amine groups). Distillation of exceeded EDA under reduced pressure (gives the purified 0 G dendrimer). The PAMAM dendrimers are shown as yellow ropy liquid.

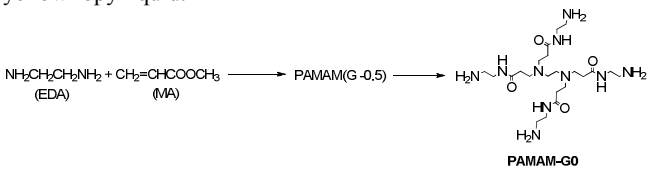

Figure 17 The reaction of molecules PAMAM-G0

(PAMAM-G0) IR (KBr) cm-1: 3325(NH), 2961, 1647(CO), 1563, 1465, 1307, 995, 687. MS (m/z):(Calculate for : 518.6 $[M+2H]^{2+}$); Found: 518.3 $[M+2H]^{2+}$

3.2 The synthesis of PNS-G0

Synthesis of 3,3',3",3'"-(ethane-1,2-diylbis(azanetriyl))tetrakis(N-(2-(((2-hydroxyl naphthalen-1-yl)methylene)amino)ethyl) propan amide) (PNS-G0).

PAMAM(G0) 0.52 g (1mmol), 2-hydroxy-1-naphthaldehyde 0.9 g (5 mmol, excessive), anhydrous sodium sulfate 0.5 g, added into 30 mL methanol. Reflux 2 h and cool to room temperature. Filtrate and washed the solid by methanol three times, vacuum drying. Got yellow brown powder about 1 g, yield 85%.

IR (KBr) cm-1: 3273 and 3064(NH), 2936, 2818, 1629(C=N), 1549, 1495, 1447, 1354, 1210, 1184, 1139, 1104, 998, 835, 739,505. ^{1}H NMR (300 MHz, DMSO-d6, δ): δ 8.95 (4H, m, H-C=N), 8.14 (4H, s, Ar-H), 8.00 (8H, d, J=6.0 Hz, Ar-H), 7.71(4H, d, N-H), 7.60(4H, m, J=6.0Hz, Ar-H), 7.38(4H, t, J=6.0 Hz, Ar-H), 7.15(4H, t, J=6.0 Hz, Ar-H), 6.71(4H, m, HO-), 3.08~4.01(24H, m, C-H), 2.17~2.27 (12H, m, C-H). ^{13}C NMR (300 MHz, DMSO-d6,δ): δ 176.9, 171.4, 160.2, 159.5, 137.0, 136.8, 134.1, 128.8, 127.8, 125.2, 125.1, 122.3, 122.1, 118.6, 118.4, 105.8, 50.3, 49.0, 40.3, 40.0, 39.7, 39.5, 39.2, 38.9, 38.6; HRMS (m/z): (Calculate for: 1134.3480 $[M+H]^+$); Found: 1134.348 $[M+H]^+$

3.3 Methods

Prepared PNS-G0 solutions in H_2O/DMSO=(99:1) at 1×10^{-6} mol/L or in DMSO at 5×10^{-5} mol/L. Take all kinds of metal ions solutions and added in PNS-G0 solutions to keep 1×10^{-4} mol/L ions concentration and form the complex solutions, which for quantitatively testing. The [Zn^{2+}] gradient concentrations solutions were prepared and added into PNS-G0 solutions for qualitatively detection. Optic test: carry the solutions by using quartz color dish and test the fluorescence emission spectra at linear light source spectrofluorometer. The up-converted fluorescence emission experiments were taken by FluoroMax-4 spectrofluorometer from excitation source xenon, continuous output, ozone-free lamp (150 W) at room temperature (~20□). The excited wavelength set at 800 nm and test ranges set from 200 nm to 850 nm, slit 3 nm.

4. Conclusions

PNS-G0 can realize up-converted fluorescence turn-on effect for high selectively qualitative and quantitative probing Zn^{2+}. This dendrimer probe based on Schiff base imine (C=N) isomerization inhibited mechanism. The organic solvent using and near two times selected sign in water/DMSO mixed solvents show the dyes need to be further modified and improved. The C=N_Zn_O fluorescence emission parts were called as Half-organic Quantum Dots (HOQDs) to give similar or new properties compared to traditional QDs. The PNS-G0 and its Zn^{2+} complex have potential applications in biological cell imaging, metal ions analytical chemistry, and up-converted optical physics areas. And the HOQDs can explore new and wide application foreground.

Notes and references

[a] *School of Chemistry and Chemical Engineering, Southeast University, Nanjing, 211189, China, TEL:+8613851438813*
E-mail: yingqian@seu.edu.cn; jiyan98@163.com

† Electronic Supplementary Information (ESI) available: [^{1}H NMR, ^{13}C NMR spectra, and HRMS of PNS-G0, MS of PAMAM-G0 list in Figure S1, Figure S2, Figure S3, and Figure S4 in the supporting file.]. See DOI: 10.1039/b000000x/

‡ Acknowledgements: The National Natural Science Foundation of China (No.61178057) and the Scientific Research Foundation of Graduate School of Southeast University (No.YBPY1209) were greatly appreciated for financial support.

1 B. L. Vallee, K. H. Falchuk, *Physiol. Rev.* 1993, **73**, 79.
2 C. J. Frederickson, J. Y. Koh, A. I. Bush, *Nat. Rev. Neurosci.* 2005, **6**, 449.
3 a) P. Saluja, V. K. Bhardwaj, T. Pandiyan, S. Kaur, N. Kaur, N. Singh, *RSC Adv.*, 2014, **4**, 9784; b) S. Y. Jiao, L. L. Peng, K. Li, Y. M. Xie, M. Z. Ao, X. Wang, X. Q. Yu, *Analyst.* 2013, **138**, 5762; c) H. Nouri, C. Cadiou, L. M. L. Daku, A. Hauser, S. Chevreux, I. D. Olivier, F. Lachaud, R. Ternane, M. T. Ayadi, F. Chuburu, G. Lemercier, *Dalton Trans.* 2013, **42**, 12157; d) Y. Mikata, A. Ugai, K. Yasuda, S. Itami, S. Tamotsu, H. Konno, S. Iwatsuki. *Chem. Biodivers.* 2012, **9(9)**, 2064; e) S. Comby, S. A.Tuck, L. K. Truman, O. Kotova, T. Gunnlaugsson, *Inorg. Chem.* 2012, **51(19)**, 10158.
4 a) H. M. Kim, M. S. Seo, M. J. An, J. H. Hong, Y. S. Tian, J. H. Choi, O. Kwon, K. J. Lee, B. R. Cho, *Angew. Chem., Int. Ed.* 2008, **47**, 5167; b) C. J. Chang, J. Jaworski, E. M. Nolan, M. Sheng, S. J. Lippard, *Proc. Natl. Acad. Sci. U.S.A.* 2004, **101**, 1129; c) H. M. Kim, B. R. Cho, *Accounts. Chem. Res.* 2009, **42**, 863.
5 J. S. Wu, W. M. Liu, J. C. Ge, H. Y. Zhang, P. F. Wang, *Chem. Soc. Rev.* 2011, **40**, 3483.

6 a) R. M. Manez, F. Sancenon, *Chem. Rev.* 2003, **103**, 4419; b) B. Valeur, I. Leray, Coord. *Chem. Rev.* 2000, **205**, 3; c) Z. C. Xu, J. Yoon, D. R. Spring, *Chem. Soc. Rev.* 2010, **39**, 1996; d) J. S. Kim, D. T. Quang, *Chem. Rev.* 2007, **107**, 3780.

7 C. Lodeiro, F. Pina, Coord. *Chem. Rev.* 2009, **253**, 1353.

8 A. P. de Silva, H. Q. N. Gunaratne, T. Gunnlaugsson, A. J. M. Huxley, C. P. McCoy, J. T. Rademacher, T. E. Rice, *Chem. Rev.* 1997, **97**, 1515.

9 Q. Zhao, F. Y. Li, C. H. Huang, *Chem. Soc. Rev.* 2010, **39**, 3007.

10 a) K. E. Sapsford, L. Berti, I. L.Medintz, *Angew. Chem. Int. Ed.* 2006, **45**, 4562; b) H. J. Carlson, R. E. Campbell, *Curr. Opin. Biotechnol.* 2009, **20**, 19.

11 W. Rettig, R. Lapouyade, *Fluorescence probes based on twisted intramolecular charge transfer (TICT) states and other adiabatic photoreactions, in Topics in Fluorescence Spectroscopy, Probe Design and Chemical Sensing*, ed. J. R. Lakowicz, Plenum Press, New York, 1994, vol. **4**, pp. 109.

12 J. F. Callan, A. P. de Silva, D. C. Magri, *Tetrahedron.* 2005, **61**, 8551

13 a) Y. N. Hong, J. W. Y. Lam, B. Z. Tang, Chem. Commun. 2009, 4332; b) M. Wang, G. X. Zhang, D. Q. Zhang, D. B. Zhu, B. Z. Tang, *J. Mater. Chem.* 2010, **20**, 1858.

14 M. Y. Berezin, S. Achilefu, *Chem. Rev.* 2010, **110**, 2641.

15 J. S. Wu, W. M. Liu, X. Q. Zhuang, F. Wang, P. F. Wang, S. L. Tao, X. H. Zhang, S. K. Wu, S. T. Lee, *Org. Lett.* 2007, **9**, 33.

16 a) W. Liu, L. Xu, R. Sheng, P. Wang, H. Li, S. Wu, *Org. Lett.* 2007, **9**, 3829; b) D. Ray, P. K. Bharadwaj, *Inorg. Chem.* 2008, **47**, 2252; c) V. Chandrasekhar, P. Bag, M. D. Pandey, *Tetrahedron.* 2009, **65**, 9876; d) H. S. Jung, K. C. Ko, J. H. Lee, S. H. Kim, S. Bhuniya, J. Y. Lee, Y. Kim, S. J. Kim, J. S. Kim, *Inorg. Chem.* 2010, **49**, 8552; e) M. Suresh, A. K. Mandal, S. Saha, E. Suresh, A. Mandoli, R. D. Liddo, P. P. Parnigotto, A. Das, *Org. Lett.* 2010, **12**, 5406; f) Z. Li, M. Yu, L. Zhang, M. Yu, J. Liu, L. Wei, H. Zhang, *Chem. Commun.* 2010, **46**, 7169.

17 a) K. E. Sapsford, L. Berti and I. L. Medintz, *Angew. Chem. Int. Ed.* 2006, **45(28)**, 4562; b) W. I. Lee, Y. Bae, A. J. Bard, *J. Am. Chem. Soc.* 2004, **126**, 8358-8359.; c) D. J. Wang, T. Imae, *J. Am. Chem. Soc.* 2004, **126**, 13204-13205; d) D. C. Wu, Y. Liu, C. B. He, S. H. Goh, *Macromolecules*, 2005, **38(24)**, 9906-9909; e) Y. F. Fan, Y. G. Fan, Y. N. Wang, *J. Appl. Polym. Sci.* 2007, **106(3)**,1640-1647; f) P. L. Wang, X. Wang, K. Meng, S. Hong, X. Liu, H. Cheng, C. C. Han, *J. Polym. Sci. Part A: Polym. Chem.* 2008, **46(10)**, 3424-3428.

18 M. J. Murcia, D. L. Shaw, E. C. Long, C. A. Naumann. *Optics Communications.* 2008, **281**, 1771

19 a) C.B. Murray, D.J. Norris, M.G. Bawendi, *J. Am. Chem. Soc.* 1993, **115**, 8706; b) A.P. Alivisatos, *Science.* 1996, **271**, 933; c) C. Donega, S.G. Hickey, S.F. Wuister, D. Vanmaekelbergh, A. Meijerink, *J. Phys. Chem. B.* 2003, **107**, 489; d) Z.A. Peng, X. Peng, *J. Am. Chem. Soc.* 2001, **123**, 183; e) R. Cohen, L. Kronik, A. Shanzer, D. Cahen, A. Liu, Y. Rosenwaks, J.K. Lorenz, A.B. Ellis, *J. Am. Chem. Soc.* 1999, **121**, 10545.

20 W.L. Wilson, P.F. Szajowski, L.E. Brus, *Science.* 1993, **262**, 1242.

21 W. Martienssen, H. Warlimont (Eds.), Springer *Handbook of Condensed Matter and Materials Data,* vol. 18, Springer Verlag,2005, p. 1120.

22 W.C.W. Chan, D.J. Maxwell, X. Gao, R.E. Bailey, M. Han, S. Nie, *Curr. Op. Biotechnol.* 2002, **13**, 40.

23 W.H. Liu, H. S. Choi, J. P. Zimmer, E. Tanaka, J. V. Frangioni, M. Bawendi, *J. Am. Chem. Soc.* 2007, **129**, 14530

24 R. C. Somers, R. M. Lanning, P. T. Snee, A. B. Greytak, R. K. Jain, M. G. Bawendi, D. G. Nocera, *Chem. Sci.* 2012, **3**, 2980

25 a) A. A. Hajaj, A. Moquin, K. D. Neibert, G. M. Soliman, F. M. Winnik, D. Maysinger, *Acs Nano.* 2011, **5(6)**, 4909; b) D. A. Geraldo, E. F. Duran-Lara, D. Aguayo, R. E. Cachau, J. Tapia, R. Esparza, M. J. Yacaman, F. D. Gonzalez-Nilo, L. S. Santos. *Anal. Bioanal. Chem.* 2011, **400**, 483.

26 a) K. A. Connors, *Binding Constants: The Measurement of Molecular Complex Stability.* John Wiley and Sons: New York, 1987.; b) S. J. K. Pond, O. Tsutsumi, M. Rumi, O. Kwon, E. Zojer, J. L. Bre´das, S. R. Marder, J. W. Perry, *J. Am. Chem. Sos.* 2004, **126**, 9291-9306; c) H. M. Kim, C. Jung, B. R. Kim, S. Y. Jung, J. H. Hong, Y.G. Ko, K. J. Lee, B. R. Cho, *Angew. Chem. Int. Ed.* 2007, **46**, 3460 -3463

27 F. Auzel, *Chem. Rev.* 2004, **104**, 139.

28 a) W. L. Peticolas, J. P. Goldsborough, K. E. J. Rieckhoff, *Phys. Rev. Lett.* 1963, **10**, 43; b) W. L. Peticolas, K. E. J. Rieckhoff, *Chem. Phys.* 1963, **39**, 1347; c) P. M. Rentzepis, C. J. Mitschele, A. C. Saxman, *Appl. Phys. Lett.* 1970, **17**, 122; d) A. C. Seldon, R. H. Coll, *Nature (London), Phys. Sci.* 1971, **229**, 210; e) J. A. Giordmaine, P. M. Rentzepis, S. L. Shapiro, K. W. Wecht, *Appl. Phys. Lett.* 1967, **11**, 216.

29 a) G. S. He, J. D. Bhawalkar, C. F. Zhao, C. K. Park, P. N. Prasad, *Opt. Lett.* 1995, **20**, 2393; b) G. S. He, C. F. Zhao, J. D. Bhawalkar, P. N. Prasad, *Appl. Phys. Lett.* 1995, **67**, 3703; c) W. Denk, J. H. Strickler, W. W. Webb, *Science*,1990, **248**, 73; d) G. S. He, L.S. Tan, Q.D. Zheng, P. N. Prasad, *Chem. Rev.* 2008, **108**, 1245.

30 F. Auzel, *Chem. Rev.* 2004, **104**, 139.

31 W. E. Case, M. E. Koch, *J. Lumin.* 1990, **45**, 351.

32 a) W. F. Hsieh, H. C. Hsu, W. J. Liao, H. M. Cheng, K. F. Lin, W. T. Hsu, C. J. Pan, *Adv. Seri. Appl. Phys.* 2011, **6**, 253-267; b) T. Yatsui, M. Ohtsu, *Reza Kenkyu*, 2011, **39(3)**, 184-187; c) C. C. Yang, *Key Eng. Mater.*, 2010, **444**, 133-162; d) X. Sun, C. G. Zhou, Mi. Xie, H. T. Sun, T. Hu, F.Y. Lu, S. M. Scott, S. M. George, J. Lian, *J. Mater. Chem. A.* 2014, **2(20)**, 7319-7326.

33 R. O. Moussodia, L. Balan, C. Merlin, C. Mustind, R. Schneider. *J. Mater. Chem.* 2010, **20**, 1147.

34 Gaussian 09, Revision A.02, M. J. Frisch, G. W. Trucks, H. B. Schlegel, G. E. Scuseria, M. A. Robb, J. R. Cheeseman, G. Scalmani, V. Barone, B. Mennucci, G. A. Petersson, H. Nakatsuji, M. Caricato, X. Li, H. P. Hratchian, A. F. Izmaylov, J. Bloino, G. Zheng, J. L. Sonnenberg, M. Hada, M. Ehara, K. Toyota, R. Fukuda, J. Hasegawa, M. Ishida, T. Nakajima, Y. Honda, O. Kitao, H. Nakai, T. Vreven, J. A. Montgomery, Jr., J. E. Peralta, F. Ogliaro, M. Bearpark, J. J. Heyd, E. Brothers, K. N. Kudin, V. N. Staroverov, R. Kobayashi, J. Normand, K. Raghavachari, A. Rendell, J. C. Burant, S. S. Iyengar, J. Tomasi, M. Cossi, N. Rega, J. M. Millam, M. Klene, J. E. Knox, J. B. Cross, V. Bakken, C. Adamo, J. Jaramillo, R. Gomperts, R. E. Stratmann, O. Yazyev, A. J. Austin, R. Cammi, C. Pomelli, J. W. Ochterski, R. L. Martin, K. Morokuma, V. G. Zakrzewski, G. A. Voth, P. Salvador, J. J. Dannenberg, S. Dapprich, A. D. Daniels, O. Farkas, J. B. Foresman, J. V. Ortiz, J. Cioslowski, and D. J. Fox, Gaussian, Inc., Wallingford CT, 2009.

35 D. A. Tomalia, H. Baker, J. Dewald, M. Hall, G. Kallos, S. Martin, J. Roeck, J. Ryder, P. Smith. *Polym. J.* 1985, **17**, 117.